



1 **Characterization of Organosulfates in Secondary**
2 **Organic Aerosol Derived from the Photooxidation**
3 **of Long-Chain Alkanes**

4
5 M. Riva¹, T. Da Silva Barbosa^{2,3}, Y.-H. Lin^{1,a}, E. A. Stone⁴, A. Gold¹, and J. D.
6 Surratt^{1,*}

7
8 ¹Department of Environmental Sciences and Engineering, Gillings School of Global Public
9 Health, The University of North Carolina at Chapel Hill, Chapel Hill, NC, USA

10 ² CAPES Foundation, Brazil Ministry of Education, Brasilia, DF 70.040-020, Brazil

11 ³Departamento de Química, Instituto de Ciências Exatas, Universidade Federal Rural do Rio
12 de Janeiro, Seropédica, Brazil

13 ⁴Department of Chemistry, University of Iowa, Iowa City, IA 52242, United States

14
15 ^a now at: Michigan Society of Fellows, Department of Chemistry, University of Michigan,
16 Ann Arbor, MI, USA

17
18 * To whom correspondence should be addressed.

19
20 Jason D. Surratt, Department of Environmental Sciences and Engineering, Gillings School of
21 Global Public Health, University of North Carolina at Chapel Hill, Chapel Hill, NC 27599
22 USA. Tel: 1-(919)-966-0470; Fax: (919)-966-7911; Email: surratt@unc.edu

23

24 The authors declare no conflict of interest.

25



26 **Abstract**

27 We report the formation of aliphatic organosulfates (OSs) in secondary organic aerosol (SOA)
28 from the photooxidation of C₁₀ – C₁₂ alkanes. The results complement those from our
29 laboratories reporting the formation of OSs and sulfonates from gas-phase oxidation of
30 polycyclic aromatic hydrocarbons (PAHs). Both studies strongly support formation of OSs
31 from gas-phase oxidation of anthropogenic precursors, hypothesized on the basis of recent
32 field studies in which aromatic and aliphatic OSs were detected in fine aerosol collected from
33 several major urban locations. In this study, dodecane, cyclodecane and decalin, considered to
34 be important SOA precursors in urban areas, were photochemically oxidized in an outdoor
35 smog chamber in the presence of either non-acidified or acidified ammonium sulfate seed
36 aerosol. Effects of chemical structure, acidity and relative humidity on OS formation were
37 examined. Aerosols collected from all experiments were characterized by ultra performance
38 liquid chromatography coupled to electrospray ionization high-resolution quadrupole time-of-
39 flight mass spectrometry (UPLC/ESI-HR-QTOFMS). Most of the OSs identified could be
40 explained by formation of gaseous epoxide precursors with subsequent acid-catalyzed
41 reactive uptake onto sulfate aerosol. The OSs identified here were also observed and
42 quantified in fine urban aerosol samples collected in Lahore, Pakistan, and Pasadena, USA.
43 Many of the OSs identified from the photooxidation of decalin and cyclodecane are isobars of
44 known monoterpene organosulfates, and thus care must be taken in the analysis of alkane-
45 derived organosulfates in urban aerosol.

46



47 **1. Introduction**

48 Atmospheric fine particulate matter (PM_{2.5}, aerosol with aerodynamic diameter ≤ 2.5
49 μm) plays a major role in scattering and absorption of solar radiation, which impacts global
50 climate (Kroll and Seinfeld, 2008; Stevens and Boucher, 2012). PM_{2.5} also participates in
51 heterogeneous chemical reactions, affecting the abundance and distribution of atmospheric
52 trace gases (Hallquist et al., 2009). Human exposure to PM_{2.5} is associated with respiratory
53 and cardiovascular diseases (Elder and Oberdorster, 2006).

54 Typically, the largest mass fraction of PM_{2.5} is organic, dominated by secondary
55 organic aerosol (SOA) formed by the oxidation of volatile organic compounds (VOCs).
56 Although SOA contributes a large fraction (20–90%, depending on location) of total PM_{2.5}
57 mass, current models predict less SOA than is generally observed during field measurements
58 (Kroll and Seinfeld, 2008; Hallquist et al., 2009). The underestimate is largely a consequence
59 of omission of intermediate volatility organic compounds (IVOC), such as alkanes or
60 polycyclic aromatic hydrocarbons (PAHs) (Pye and Pouliot, 2012; Tkacik et al., 2012) as
61 SOA precursors. Long-chain alkanes are important anthropogenic pollutants emitted by
62 combustion and vehicular sources representing up to 90% of the anthropogenic emissions in
63 certain urban areas (Fraser et al., 1997, Gentner et al., 2012). In the atmosphere, they are
64 rapidly depleted by reaction with OH and NO₃ radicals (Atkinson, 2000) yielding a large
65 variety of oxygenated compounds (Lim and Ziemann, 2005; 2009; Yee et al., 2012), which
66 could lead to SOA formation (Lim and Ziemman, 2009; Loza et al., 2014). SOA yields have
67 been measured for C₇-C₂₅ alkanes having linear, branched and cyclic structures (Lim and
68 Ziemman, 2009; Presto et al., 2010; Loza et al., 2014; Hunter et al., 2014). Structure plays a
69 key role in SOA yield, which increases with carbon number or the presence of cyclic features
70 and tends to decrease with branching as gas-phase fragmentation predominates (Carrasquillo
71 et al., 2014; Loza et al., 2014; Hunter et al., 2014).



72 The presence of organosulfates (OSs) has been demonstrated in several atmospheric
73 compartments, including atmospheric aerosol (Iinuma et al., 2007; Gómez-González et al.,
74 2008; Hawkins et al., 2010; Hatch et al., 2011; Kristensen et al., 2011; Stone et al., 2012;
75 Shalamzari et al., 2013; Hansen et al., 2014; Liao et al., 2015), rain (Altieri et al., 2009),
76 clouds and fog (Pratt et al., 2013; Boone et al., 2015) and several studies indicate that OSs
77 could contribute a substantial fraction (up to 30%) of the organic mass measured in ambient
78 PM_{2.5} (Surratt et al., 2008; Tolocka and Turpin, 2012).

79 Although the variety of OSs identified from field measurements is quite large (Surratt
80 et al., 2008; Tao et al., 2014; Kuang et al., 2015; Wang et al., 2015), only a few OS precursors
81 have been unequivocally identified through laboratory studies. OSs have been generated in
82 SOA in smog chambers from OH, NO₃ or O₃ oxidation of BVOCs, including isoprene (Surratt
83 et al., 2007, Ng et al., 2008), 2-methyl-3-buten-2-ol (MBO) (Zhang et al., 2012; Mael et al.,
84 2015), unsaturated aldehydes (Schindelka et al., 2013; Shalamzari et al., 2014; Shalamzari et
85 al., 2015), monoterpenes (Iinuma et al., 2007; Iinuma et al., 2009; Surratt et al., 2008), and
86 sesquiterpenes (Liggio et al., 2006; Surratt et al., 2008; Iinuma et al., 2009; Noziere et al.,
87 2010; Chan et al., 2011) in the presence of acidified sulfate aerosol. However, the large
88 number of unidentified OSs having C₂ to C₂₅ skeletons observed in recent field studies are
89 clearly not derived from BVOC precursors, and suggest alkanes and aromatics as a major
90 source of hitherto unrecognized of OS precursors (Tao et al., 2014; Kuang et al., 2015; Wang
91 et al., 2015). Ma et al. (2014) have recently shown that the contribution of aromatic OSs could
92 represent up to two-thirds of the OSs identified in Shanghai. Aliphatic OSs were identified in
93 the ambient samples from urban locations (Tao et al., 2014; Kuang et al., 2015; Wang et al.,
94 2015), suggesting that gas-phase oxidation of long-chain or cyclic alkanes could be an
95 important source of OSs (Tao et al., 2014). At present, lack of authentic standards currently



96 prevents quantitation of the OSs contribution to PM_{2.5} mass, underscoring the need to better
97 identify the OS precursors.

98 Studies on the impact of NO_x and O₃ on SOA formation from oxidation of long-chain
99 alkanes (Loza et al., 2014; Zhang et al., 2014) have shown that the presence of NO_x tends to
100 reduce SOA formation by reaction of peroxy radicals (RO₂) with NO, to yield alkoxy radicals
101 (RO). For alkanes containing fewer than 10 carbons, the fragmentation/decomposition of RO
102 radicals will produce higher volatility species (e.g., small carbonyls), which suppresses or
103 reduce SOA formation (Lim and Ziemann, 2005, 2009). Recent studies have shown that
104 increased aerosol acidity is a key variable in enhancing SOA formation through acid-
105 catalyzed reactive uptake and multiphase chemistry of oxidation products derived from
106 biogenic VOCs (BVOCs) such as isoprene (Surratt et al., 2010) and α -pinene (Iinuma et al.,
107 2009); however, no such studies have been reported for the oxidation of alkanes. Formation of
108 highly oxidized products, including OSs, demonstrates the importance of heterogeneous
109 processes, such as reactive uptake of epoxides onto acidic sulfate aerosol, in SOA formation
110 (Iinuma et al., 2009; Surratt et al., 2010; Chan et al., 2011; Lin et al., 2014; Shalamzari et al.,
111 2015). OSs may also be formed by either nucleophilic substitution of organic nitrates by
112 sulfate (Darer et al., 2011; Hu et al., 2011) or by heterogeneous oxidation of unsaturated
113 compounds involving sulfate anion radicals (Noziere et al., 2010; Schindelka et al., 2013;
114 Schone et al., 2014).

115 Formation of OSs from the gas-phase oxidation of the C₁₀ alkanes, cyclodecane
116 (C₁₀H₂₀) and decalin (bicyclo[4.4.0]decane; C₁₀H₁₈), and C₁₂ alkane, dodecane (C₁₂H₂₆), in
117 the presence of sulfate aerosol under varying acidities is reported in this work. Effects of RH,
118 aerosol acidity and alkane structures on OS formation were investigated. SOA collected from
119 outdoor smog chamber experiments was chemically characterized by ultra performance liquid
120 chromatography interfaced to high-resolution quadrupole time-of-flight mass spectrometry



121 equipped with electrospray ionization (UPLC/ESI-HR-QTOFMS). In addition, effect of
122 solvent mixture (methanol vs acetonitrile/toluene) on OS quantification was investigated.
123 Finally, PM_{2.5} samples collected from Lahore, Pakistan and Pasadena, USA were analyzed to
124 detect and quantify OSs identified from the smog chamber experiments.

125

126 **2. Experimental**

127 **2.1 Chamber Experiments.** Eighteen experiments were performed at the University of
128 North Carolina (UNC) outdoor smog chamber facility located at Pittsboro, NC. Details of this
129 facility have been previously described (Lee et al., 2004; Kamens et al., 2011). Briefly, it is a
130 274-m³ dual chamber divided into two sides by a Teflon film curtain. One side referred as
131 “North Chamber” has an actual volume of 136 m³, and the other side referred as “South
132 Chamber” has an actual volume of 138 m³. Prior to each experiment, both sides of the
133 chamber were flushed using rural background air using an exhaust blower for at least 12
134 hours. Clean air was then injected into both sides of the chamber using a clean air generator to
135 reduce concentrations of background aerosol and VOCs. Experiments were performed under
136 two humidity conditions: at low RH (10–20%) and high RH (4–60%). For experiments
137 conducted at low RH (i.e., dry), the clean air generator was used after the preliminary venting
138 using rural air for approximately 48–72 hours. A scanning mobility particle sizer (SMPS, TSI
139 3080) was used to measure aerosol size distributions, including number and volume
140 concentrations inside both chambers. Before each experiment, the typical aerosol mass
141 concentration (assuming an aerosol density of 1 g cm⁻³) background was less than ~ 3 μg m⁻³
142 in humid conditions and less than ~ 0.2 μg m⁻³ for dry experiments. Either non-acidified or
143 acidified ammonium sulfate seed aerosols were introduced into the chambers by atomizing
144 aqueous solutions of 0.06 M (NH₄)₂SO₄ or 0.06 M (NH₄)₂SO₄ + 0.06 M H₂SO₄, respectively.
145 After 15 min of atomization, ~ 40 μg m⁻³ of seed aerosol was injected into the chambers.



146 After stabilization of aerosol volume concentrations, Teflon filters were collected (47 mm
147 diameter, 1.0 μm pore size, Tisch Environmental, EPA PM_{2.5} membrane) over 45 min at a
148 sampling rate of $\sim 25 \text{ L min}^{-1}$ in order to measure baseline aerosol composition prior to
149 injection of the SOA precursors. None of the aliphatic OSs produced from the oxidation of
150 studied alkanes were detected in the chamber background. Dodecane (Sigma-Aldrich, 99%),
151 cyclodecane (TCI, 94%) or decalin (Sigma-Aldrich, 99%, mixture of *cis* + *trans*) were
152 introduced into both sides of the chamber by passing a N₂ flow through a heated manifold
153 containing a known amount of liquid compound. Concentrations of alkanes were measured
154 online in each side every 10 minutes by a gas chromatograph with a flame ionization detector
155 (GC-FID, Model CP-3800, Varian), calibrated before each experiment with a standard
156 mixture of hydrocarbons. Isopropyl nitrite (IPN) (Pfaltz & Bauer, 97%) was used as an OH
157 radical precursor (Raff and Finlayson-Pitts, 2010) and was injected into both sides when VOC
158 signals were stable as measured by the GC-FID. O₃ and NO_x concentrations were monitored
159 using UV photometric and chemiluminescent analyzers, respectively (O₃: Model 49P,
160 Thermo-Environmental; NO_x: Model 8101B, Bendix). Both instruments were calibrated as
161 described in previous work (Kamens et al., 2011). Dilution rate for each chamber was
162 monitored by sulfur hexafluoride (SF₆) measured using gas chromatography with electron
163 capture detection (GC-ECD). RH, temperature, irradiance and concentration of O₃ and NO_x
164 were recorded every minute. SOA formation from alkane photooxidation was monitored for
165 all experiments. 2–3 hours following IPN injection, which corresponds to the end of SOA
166 growth as measured by the SMPS, filter sampling was initiated. For each experiment, two
167 filters from each side of the chamber were collected for 45 min – 2 hours (sampling rate ~ 25
168 L min⁻¹) to characterize particle-phase reaction products. Based on SOA volume
169 concentrations measured by the SMPS, sampling time was adjusted to obtain an SOA mass of
170 about $\sim 100 \mu\text{g}/\text{filter}$. Experimental conditions are summarized in Table 1.



171 **2.2 Ambient Aerosol Collection.** Five filters collected in Lahore (Pakistan) between January
172 2007 and January 2008 (Stone et al., 2010) and eight filters collected in Pasadena (USA)
173 during the 2010 California Research at the Nexus of Air Quality and Climate Change
174 (CalNex) field study from 15 May – 15 June 2010 (Hayes et al., 2013), were analyzed for the
175 OSs identified in smog chamber experiments. PM_{2.5} was collected on prebaked quartz fiber
176 filters (QFF, Pall Life Sciences, Tissuquartz, 47 mm for Lahore, 20.3 cm × 25.4 cm for
177 Pasadena) using a medium-volume sampling apparatus at Lahore (URG-3000, Chapel Hill,
178 NC, USA) and a high-volume sampler (Tisch Environmental, Cleves, OH, USA) at Pasadena.
179 As stipulated previously at both urban sites, anthropogenic activities (e.g., vehicular exhaust,
180 industrial sources, cooking, etc.) likely dominated the organic aerosol mass fraction of PM_{2.5}
181 (Stone et al., 2010; Hayes et al., 2013).

182 **2.3 Filter Extraction.** The impact of the solvent mixture on OS quantification was also
183 explored in this work. Filters collected from smog chamber experiments were extracted using
184 two different solvent mixtures. One filter was extracted using 22 mL of high-purity methanol
185 (LC-MS CHROMASOLV-grade, Sigma-Aldrich, ≥ 99.9 %) under 45 min (25 min + 20 min)
186 of sonication at room temperature while the second filter was extracted using 22 mL of a
187 70/30 (v/v) solvent mixture containing acetonitrile/toluene (CHROMASOLV-grade, for
188 HPLC, Sigma-Aldrich, ≥ 99.9 %). Extracts were then blown dry under a gentle nitrogen
189 stream at ambient temperature (Surratt et al., 2008; Zhang et al., 2011; Lin et al., 2012). Dry
190 extracts were then reconstituted with 150 μL of either a 50:50 (v/v) solvent mixture of
191 methanol and water (MilliQ water) or a 50:50 (v/v) solvent mixture of acetonitrile and water.
192 Filters collected from field studies were extracted using methanol as solvent mixture and
193 following the protocol described above; however, prior to drying, extracts were filtered
194 through 0.2-μm PTFE syringe filters (Pall Life Science, Acrodisc) to remove insoluble
195 particles or quartz filter fibers.



196 **2.4 Chemical Analysis.** Characterization of OSs in chamber experiments was performed
197 using ultra performance liquid chromatography interfaced to a high-resolution quadrupole
198 time-of-flight mass spectrometer equipped with an electrospray ionization source (UPLC/ESI-
199 HR-Q-TOFMS, 6500 Series, Agilent) operated in the negative ion mode. Exact operating
200 conditions have been previously described (Lin et al., 2012). 5 μL sample aliquots were
201 injected onto a UPLC column (Waters ACQUITY UPLC HSS T3 column). Octyl sulfate
202 ($\text{C}_8\text{H}_{17}\text{O}_4\text{S}^-$; Sigma-Aldrich) and 3-pinanol-2-hydrogen sulfate ($\text{C}_9\text{H}_{13}\text{O}_6\text{S}^-$) were used as
203 surrogate standards to quantify the identified aliphatic OSs.

204

205 **3. Results and Discussion**

206 In the subsequent sections, detailed chemical characterization of OSs identified from the gas-
207 phase oxidation of dodecane, decalin and cyclodecane in the presence of ammonium sulfate
208 aerosol is presented. The presence of OSs was revealed by the appearance of characteristic
209 fragment ions at m/z 79.95 ($\text{SO}_3^{\cdot-}$), 80.96 (HSO_3^-) and/or 96.96 (HSO_4^-) in tandem mass
210 spectra (MS^2) (Iinuma et al., 2007; Gómez-González et al., 2008; Surratt et al., 2008;
211 Shalamzari et al., 2013; 2014). Tentative structures, retention times and exact mass
212 measurements of OSs detected in this work are reported in Table S1. The low abundance of
213 some OSs precluded acquisition of high-resolution MS^2 data, and thus, structures have not
214 been proposed for these less-abundant parent ions.

215 **3.1 Characterization of OSs from Dodecane Photooxidation.** Seven OSs, including
216 isobaric compounds, were identified in SOA produced from the gas-phase oxidation of
217 dodecane in the presence of sulfate seed aerosol. None have previously been reported in
218 chamber experiments, although they have recently been observed in ambient fine aerosol
219 samples (Tao et al., 2014; Kuang et al., 2015). Concentrations of the products are reported in
220 Table S2. Three isobaric parent ions with m/z 279 ($\text{C}_{12}\text{H}_{23}\text{O}_5\text{S}^-$, 279.1254) were identified in
221 SOA generated from dodecane oxidation in the presence of acidified ammonium sulfate



222 aerosol. Based on Yee et al. (2012; 2013) the products are tentatively assigned as 1,3-
223 dodecanone sulfate isomers. The MS² spectra of the products were identical, having product
224 ions diagnostic for a sulfate ester β to an abstractable proton (Surratt et al., 2008; Gómez-
225 González et al., 2008) at *m/z* 199 (C₁₂H₂₃O₂⁻, loss of neutral SO₃) and 97 (HSO₄⁻), precluding
226 assignment of positional isomerism. A study on the OH oxidation of the linear alkane
227 octacosane indicates a strong preference for oxidation at terminal carbons, with the C₂
228 carbonyl predominating (Ruehl et al., 2013), suggesting the structure 2-dodecanone-4-sulfate
229 for OS-279 and possibly 3-dodecanone-5-sulfate and 4-dodecanone-6-sulfate isomers as
230 isobaric ions. Figures 1 and S1 present the MS² spectrum of OS-279 and proposed
231 fragmentation pathway, respectively. By chemical ionization mass spectrometry (CIMS)
232 operating in the negative mode, Yee et al. (2012) identified the formation of hydroperoxides
233 from the oxidation of dodecane under low-NO_x conditions, confirming the predicted RO₂ –
234 HO₂ reaction pathway in the low-NO_x regime. First-generation hydroperoxides can react with
235 OH by further oxidation to form low-volatility, more highly oxidized products or by
236 fragmentation/decomposition of alkoxy (RO) radicals to form products with higher volatility
237 (Yee et al., 2012, Carrasquillo et al., 2014). In our study, OH radicals were formed from IPN
238 photolysis without additional injection of NO. Under these conditions, RO₂ chemistry is
239 dominated by RO₂ + HO₂ and/or RO₂ + RO₂ reactions as discussed by Raff and Finlayson-
240 Pitts (2010). Although RO₂ radicals formed in the first oxidation step could also react with
241 NO formed by IPN photolysis, significant formation of ozone under chamber conditions (0.3-
242 0.6 ppm, depending on concentration of IPN injected) would rapidly quench NO. Thus RO₂ +
243 NO reactions are not anticipated to be significant (Raff and Finlayson-Pitts, 2010). Carbonyl
244 hydroperoxide (CARBROOH), which has been identified in the gas phase by Yee et al.
245 (2012), is likely involved in acid-catalyzed reactive uptake onto sulfate aerosol.
246 Heterogeneous chemistry of gas-phase organic peroxides has been previously suggested to



247 explain the formation of certain OSs and tetrols (Claeys et al., 2004; Riva et al., 2015b). Acid-
248 catalyzed perhydrolysis of hydroperoxides followed by reaction with sulfate anion radicals
249 could also be possible route to the formation of OS-279 (Figure 1). However, further
250 investigation is required to better understand how acidified sulfate seed aerosol takes up
251 organic peroxides from the gas phase and how particle-phase reactions might degrade organic
252 peroxides into OSs.

253 **3.2 Characterization of OSs from Decalin Photooxidation.** Gas-phase oxidation of cyclic
254 alkanes at room temperature and atmospheric pressure has received less attention than linear
255 or branched alkanes. However, recent studies have demonstrated that oxidations of cyclic
256 alkanes by OH radicals produce less-volatile oxygenated compounds and have larger SOA
257 yields (Yee et al., 2013; Hunter et al., 2014). Significant formation of OSs (up to $1 \mu\text{g m}^{-3}$)
258 and SOA were observed in all experiments of decalin photooxidation (Tables 1 and S3),
259 revealing the high potential for bicyclic alkanes to form OSs. All OSs (25 OSs including
260 isomeric/isobaric structures) identified from the oxidation of decalin in the presence of
261 ammonium sulfate aerosol have been observed in ambient aerosol, underscoring the potential
262 importance of alkanes to OS formation in urban areas (Tao et al., 2014; Kuang et al., 2015;
263 Wang et al., 2015). MS^2 spectra were obtained for all OSs identified from decalin oxidation,
264 except for parent ions at m/z 195.0697 (OS-195) and 299.0805 (OS-299). All of the parent
265 ions show an intense product ion at m/z 96.96, indicative of an aliphatic sulfate ester.
266 Retention times and tentative structural assignments are given in Table S1.

267 Figures 2 and S2 present MS^2 spectra and fragmentation schemes of selected parent
268 ions at m/z 265.0749 (OS-265), 269.0696 (OS-269), 295.0494 (OS-295) and 326.0554 (OS-
269 326). MS^2 spectra and fragmentation schemes of other OSs are reported in Figure S3-S7.
270 These selected OSs exhibit specific fragmentation patterns and were, as described in the next
271 section, quantified and characterized in the fine urban aerosol samples. Four isomers of OS-



272 265 with composition $C_{10}H_{17}O_6S^-$ were identified in decalin-derived SOA collected from all
273 experiments. With regard to components of ambient SOA, it is important to mention that the
274 formation of isobaric OSs with the same elemental composition of $C_{10}H_{17}O_6S^-$ isobars have
275 also been previously identified in SOA produced from the gas-phase oxidation of
276 monoterpenes (Liggio et al., 2006; Surratt et al., 2008) and are not unique to decalin
277 oxidation. The product ion at nominal m/z 97 (HSO_4^-) and loss of neutral SO_3 in the MS^2
278 spectrum (Figure 2a) is consistent with an aliphatic OS having a labile proton in a β position
279 (Attygalle et al., 2001). Absence of product ions corresponding to a loss of a terminal
280 carbonyl ($-CO$) or a carboxyl group ($-CO_2$), respectively (Romero and Oehme, 2005;
281 Shalamzari et al., 2014), and a composition corresponding to 2 double bond equivalencies
282 (DBEs) has thus been attributed to an internal carbonyl group and a six-membered ring. A
283 scheme leading to the structure proposed in Figure 2a is based on the abstraction of H at the
284 ring fusion and C_1-C_2 bond cleavage (Figure S8, pathway a) and subsequent reaction with O_2
285 followed by 1,5-H shifts leading to an epoxide and sulfate ester by reactive
286 uptake/heterogeneous chemistry.

287 The composition of the parent ion at m/z 269.0696 ($C_9H_{17}O_7S^-$) corresponds to one
288 DBE. MS^2 spectrum yields products consistent with a sulfate ester β to an abstractable proton
289 and similar to OS-265, neither a terminal carbonyl nor a carboxyl functional group was
290 detected in the OS-269. As a result, the presence of hydroperoxide and/or hydroxyl
291 substituents is expected in order to help explain this molecular formula obtained from the
292 accurate mass measurement. In Figure 3, tentative pathways leading to the formation of OS-
293 267, OS-269 and OS-285 are proposed. Under low- NO_x conditions abstraction of a proton α
294 to the ring fusion of decalin followed by reaction with O_2 leads to the 1-hydroperoxy radical
295 (Yee et al., 2013; Schilling Fahnstock et al., 2015), which in turn can react with another RO_2
296 radical to yield the corresponding alkoxy radical ($C_{10}H_{17}O^*$) (Atkinson, 2000). Cleavage of



297 the C₁–C₂ decalin bond, followed by reaction with a second O₂ molecule and HO₂ leads to a
298 terminal carbonyl hydroperoxide (tCARBROOH; C₁₀H₁₈O₃). As reported in recent studies,
299 the resulting RO₂ radical can undergo isomerization/auto-oxidation to yield a hydroperoxide
300 (Ehn et al., 2014; Jokinen et al., 2014; Mentel et al., 2015), which can lead to the formation of
301 OSs through reactive uptake (Mutzel et al., 2015). By analogy to other aldehydes, OH
302 preferentially abstracts the tCARBROOH aldehydic H (79:21 branching ratio; Kwok and
303 Atkinson 1995). The RO₂ radical produced from H-atom could react with RO₂ or HO₂ and
304 form an acyl-oxy radical (R(O)O*), which decarboxylates quickly (Chacon-Madrid et al.,
305 2013) to a hydroperoxyperoxy radical (C₉H₁₇O₄*). The hydroperoxyperoxy radical can react
306 via pathway **a** (Figure 3) leading to OS-267, previously unreported, or OS-269 or pathway **b**
307 (Figure 3) leading to OS-285. Pathway **a** proceeds via a 1,7-H shift followed by elimination
308 of OH from the resulting dihydroperoxy alkyl radical to give a dihydroperoxyepoxide by a
309 1,5-H shift and OH elimination analogous to the formation of isoprene epoxydiol (IEPOX)
310 (Paulot et al., 2009; Mael et al., 2015). The epoxide can then undergo acid-catalyzed ring
311 opening to give OS-269, which may be further oxidized to OS-267. The MS² spectrum of OS-
312 285 (Figure S5) shows product ions corresponding to HSO₃⁻, HSO₄⁻ and loss of neutral SO₃,
313 in accord with a sulfate ester β to a labile proton, but yields no further structural information.
314 The structure proposed for OS-285 is based on the reaction of the hydroperoxyperoxyl radical
315 intermediate in pathway **a** with RO₂ followed by a 1,6-H shift and addition of O₂ to give a
316 hydroxyhydroperoxyperoxyl radical (C₉H₁₇O₅*) leading to an epoxide by a 1,5-H shift and
317 OH elimination as described above (Iinuma et al., 2009; Surratt et al., 2010; Jacobs et al.,
318 2013; Mael et al., 2015).

319 In Figure 4, pathways from an initial 1-peroxy transient are proposed to products
320 designated OS-295, OS-311 and OS-326. Three isobaric ions corresponding to OS-295
321 (C₁₀H₁₅O₈S⁻) were identified in decalin-derived SOA under all experimental conditions.



322 Figure 2c shows the MS² spectrum of the parent ion at m/z 295. A product ion at m/z 251
323 corresponding to loss of CO₂ (Romero and Oehme, 2005; Shalamzari et al., 2014) is present
324 in addition to product ions consistent with a sulfate ester β to a labile H (Riva et al., 2015b).
325 Pathway **a** leads to the structure consistent with the MS² spectrum and 3 DBEs required by
326 the composition of the parent ion. The salient features of pathway **a** include oxidation of the
327 RO₂ to 2-decalinone, formation of a C₁₀ alkoxy radical followed by ring cleavage of the
328 C₉–C₁₀ decalin bond leading to a 4-(carboxy cyclohexyl)-1-hydroperoxybut-2-yl radical via
329 RO₂ chemistry, and a 1,7-H shift and acid-catalyzed ring opening of the epoxide resulting
330 from the addition/isomerization of the O₂ adduct (Paulot et al., 2009).

331 Two isobaric parent ions with identical MS² spectra were observed at m/z 311 (Figure
332 S7). The only observed product ion at m/z 97 is consistent with a sulfate ester, but not
333 informative with regard to a more refined assignment of molecular structure. Pathway **b** to a
334 hydroperoxide for the parent ion with 3 DBEs is proposed by analogy to the putative
335 hydroperoxide structures of OS-267, OS-269 and OS-285. Pathway **b** is characterized by a H-
336 abstraction from a carbon at the ring fusion of 2-decalinone leading to formation of an 2-
337 decalinone-6-oxyl radical followed by a sequence of ring cleavage, O₂ additions and H-shifts
338 to form a 4-(2,6-cyclohexyl)-2-hydroperoxybutan-1-oxide that can form the sulfate ester on
339 reactive uptake. Abstraction of H₁ rather than H₆ would lead to an isobaric structure.

340 Four isobaric ions corresponding to C₁₀H₁₆NO₉S⁻ with identical MS² spectra (Figure
341 1d) were detected at nominal mass m/z 326. The loss of 63 mass units as neutral HNO₃
342 (Figure S2d) is in accord with a nitrate ester (Surratt et al., 2008), supported by the absence of
343 product ions from loss of NO or NO₂ (Kitanovski et al., 2012). Pathway **c**, to the parent ion at
344 m/z 326 proceeds from the reaction of the decalin-2-peroxy radical with NO to form decalin-
345 2-nitrate (C₁₀H₁₇NO₃) (Atkinson, 2000). From this point, a sequence of reactions identical to
346 pathway **b** yields the parent OS-326. It is important to mention that the formation of isobaric



347 OSs with the same elemental composition of $C_{10}H_{16}NO_9S^-$ isobars have also been identified
348 in SOA produced from the gas-phase oxidation of monoterpenes (Surratt et al., 2008).

349 The MS^2 spectrum for the single parent ion at m/z 281 corresponding to the
350 composition $C_{10}H_{17}O_7^-$ (OS-281) gave product ions expected for a sulfate ester β to a labile
351 proton with 2 DBE, but no additional structural information (Figure S4). The pathway
352 proposed in Figure S8 pathway **b** is based on gas-phase oxidation of to a 4-(cyclohexan-2-
353 one)but-1-yl radical followed by reaction with O_2 and a 1,6-H shift followed by addition of a
354 second O_2 , a 1,5-H shift and elimination of OH to give an epoxide. The direction of ring
355 opening of the internal epoxide by reactive uptake to give the final product is arbitrary. Three
356 isobaric parent ions at m/z 297 corresponding to the composition $C_{10}H_{17}O_8S^-$ with 2 DBEs
357 were identified. Loss of water, HSO_4^- and SO_3 as a neutral fragment in the MS^2 spectrum of
358 the major isobar (OS-297) is consistent with a hydroxyl-substituted sulfate ester β to a labile
359 proton (Figure S6). The scheme proposed in Figure S8 pathway **c** is based on the oxidation to
360 a 4-(cyclohexan-2-one)but-1-yl radical as in pathway **b**. However, in contrast to pathway **b**,
361 RO_2 formed by the addition of O_2 undergoes a 1,6-H shift followed by addition of a second
362 O_2 molecule, a 1,5-H shift and elimination of OH to yield an epoxide, which be reactively
363 taken up to give a sulfate ester. The direction of ring opening of the internal alkyl epoxide is
364 arbitrary.

365 **3.3 Characterization of OSs from Cyclodecane Photooxidation.** The concentrations of
366 OSs identified from gas-phase oxidation of cyclodecane are reported in Table S4. High levels
367 of OSs were observed in experiments performed under dry conditions with acidified
368 ammonium sulfate seed aerosol. The impact of acidity on OS formation will be discussed in
369 more detail in the following section. The MS^2 spectra of all cyclodecane products show only a
370 single product ion at nominal m/z 97 corresponding to bisulfate (Figures S9 – S13), indicating
371 that the oxidation products are sulfate esters β to a labile proton. None of the fragment ions



372 observed in the MS² spectrum suggests neither a terminal carbonyl nor a carboxyl functional
373 group are present in the cyclodecane-OSs, consistent with retention of the cyclodecane ring
374 the oxidation products. Tentative structures proposed in Table S1 are based on DBE
375 calculations and retention of the cyclodecane ring supported by MS² data. Pathways proposed
376 in Figures S14 and S15 are initiated by H-abstraction and based on reaction sequences for
377 which precedent has been established: addition of O₂ to cycloalkyl radicals to give RO₂ which
378 either react with RO₂ to yield alkoxy radicals (Atkinson, 2000; Yee et al., 2012) or undergo
379 intramolecular H-shifts leading to generation of hydroperoxydes (Ehn et al., 2014; Jokinen et
380 al., 2014). The formation of compounds such as cyclodecanone (C₁₀H₁₈O) or cyclodecane
381 hydroperoxide (C₁₀H₂₀O₂) are proposed as intermediate products leading to epoxy-
382 compounds after additional oxidation/isomerization processes, as presented in Figures S14
383 and S15. Since authentic standards are unavailable and the MS² data do not allow specific
384 structural features to be assigned, the end products in pathways in Figures S14 and S15 are
385 arbitrary. Isobars may be explained by *cis/trans* epoxide ring opening or the span of an H-
386 shift (1,5-,1,6- and 1,7-H shifts are possible). In the case of OS-249, where *cis/trans* isomers
387 are not possible; the two isobaric structures may result from different H-shifts. OS-265 and
388 OS-281 are reported here for the first time in chamber studies.

389 **3.4 Effect of Alkane Structure on Relative SOA Yield.** Alkane structures appear to be
390 important determinants of the relative yields of OSs from dodecane, decalin and cyclodecane
391 photooxidation. Tables S2-S4 show that OS concentrations are significantly higher from the
392 photooxidation of decalin and cyclodecane than from dodecane. As reported in Table 1, SOA
393 formation from gas-phase oxidation of decalin and cyclodecane was much higher than during
394 photooxidation of dodecane, which could explain the larger amount of OSs identified.
395 Although the SOA formed from photooxidation of both cyclic alkanes was comparable, the



396 sum of OSs quantified from oxidation of decalin was 3-4 times higher. An investigation of the
397 reason for these differences is ongoing.

398 **3.5 Impact of Relative Humidity and Acidity on OS Formation.** Experiments were
399 performed under conditions reported in Table 1. As shown in Figure 5 and Tables S2-S4, the
400 presence of acidic aerosols significantly increases OS formation in most cases, as previously
401 observed for OSs in SOA generated from biogenic sources (Iinuma et al., 2007; Surratt et al.,
402 2007; Chan et al., 2011). Since differences in meteorology could impact experimental results
403 from the outdoor chamber, caution must be exercised in comparing experiments performed on
404 different days. However, same-day, side-by-side experiments allow for clear resolution of the
405 effects of aerosol acidity and seed composition on OS formation. When comparing
406 experiments performed under dry versus wet conditions with acidified ammonium sulfate
407 aerosol, higher RH conditions significantly reduce OS formation, likely attributable to an
408 increase in pH because of dilution by additional particle water. To better investigate the effect
409 of acidity on OS formation, products were divided in two groups (Figure 5), those whose
410 concentrations were increased by a factor ≥ 2 (Group-1) and ≤ 2 (Group-2). Figure 5 and
411 Tables S2-S4 show that OSs identified from dodecane photooxidation belong to Group-2,
412 with the exception of OS-279. OSs from decalin photooxidation, including OS-195, OS-269
413 and OS-297 belong to Group-2 as well. OSs can be formed via different pathways, including
414 acid-catalyzed ring-opening reactions of epoxy-containing SOA constituents, reactive uptake
415 of unsaturated compounds into the particle phase, or by reaction with the sulfate anion radical
416 (Rudzinski et al., 2009; Nozière et al., 2010; Schindelka et al., 2013; Schöne et al., 2014).
417 OSs may also result from nucleophilic substitution of nitrate by sulfate (Darer et al., 2011; Hu
418 et al., 2011). The impact of acidity on OS formation arising from the different pathways has
419 been investigated principally for reactive uptake of epoxy-compounds (Jacobs et al., 2013;
420 Lin et al., 2012; Gaston et al., 2014; Riedel et al., 2015) for which OS formation is strongly



421 enhanced under acidic conditions (Lin et al. (2012)). However, a similar enhancement was not
422 observed in our study on PAH-OSs, which were not expected to result from epoxide
423 chemistry (Riva et al., 2015a). Based on these observations, the formation of Group-1 OSs are
424 hypothesized to be products of reactive uptake of gas-phase epoxides.

425 **3.6 Impact of Solvent Mixture on OS Quantification.** Additional filters were collected from
426 each side of the outdoor chamber and for each experiment to investigate the impact of solvent
427 mixture on OS quantification. Tao et al. (2014) have recently reported that less polar solvents
428 such as an acetonitrile (ACN)/toluene mixture are a better choice for extraction of long alkyl-
429 chain OSs from filters using a nanospray-desorption electrospray ionization mass
430 spectrometry where the extraction occurs *in situ* and the analyses are qualitative. Figure 6
431 demonstrates that, overall, concentrations of OSs (ng m^{-3}) from the photooxidation of
432 dodecane, decalin and cyclodecane seem to be more efficiently extracted by the ACN/toluene
433 mixture. Tables S2-S4, showing the ratios of the concentrations individual OSs extracted by
434 the ACN/toluene mixture divided by the concentration of OSs extracted by methanol,
435 indicates that all C_{10} - and C_{12} - OS products, including highly oxidized OS, appear more
436 efficiently extracted by the ACN/toluene mixture. For OSs smaller than C_{10} , extraction
437 efficiencies are about the same. As noted above, isobars of OSs identified from the oxidation
438 of alkanes have been observed in SOA generated from the oxidation of monoterpenes that are
439 currently used as tracers for monoterpene SOA chemistry (Hansen et al., 2014; Ma et al.,
440 2014). Hence, in addition to the caution that quantitation of alkane and monoterpene OSs is
441 uncertain in the absence of authentic standards, some monoterpene OSs may be
442 underestimated if not fully extracted because most studies use methanol as an extraction
443 solvent (Surratt et al., 2008; Iinuma et al., 2009). More work is, however, needed to better
444 characterize and elucidate the impact of solvent on the quantitation of biogenic and
445 anthropogenic OSs, especially compounds $> \text{C}_{10}$.



446 **3.7 OSs Derived from Long-Chain Alkanes in Ambient Fine Urban Aerosol.** Archived
447 fine urban aerosol samples collected at Lahore, Pakistan, and Pasadena, USA were used to
448 evaluate and quantify OSs identified in SOA produced from the photooxidation of long-chain
449 alkanes. Filters were initially extracted using methanol and comparison to OSs quantified
450 using another solvent mixture was not possible. As previously mentioned, seven parent ions
451 have been observed in laboratory studies. Therefore, extracted ion chromatograms (EICs)
452 obtained from smog chamber experiments were compared to those obtained from both urban
453 locations to confirm that observed OSs correspond to OSs identified in our lab study. Figures
454 7 and S16 present the EICs of OSs observed in both ambient and our smog chamber-
455 generated SOA. Table 2 identifies 12 OSs, along with concentrations, present in PM_{2.5}
456 collected from Lahore, Pakistan and Pasadena, USA and also observed in our smog-chamber-
457 generated SOA.

458 The high concentrations, especially at Lahore (Pakistan) of the OSs measured in the
459 ambient aerosol samples support their use as tracers for SOA produced from the oxidation
460 long-chain alkanes in urban areas. This is consistent with recent proposals (Tao et al., 2014).
461 OS-195 (C₇H₁₅O₄S⁻), OS-249 (C₁₀H₁₇O₅S⁻), OS-255 (C₉H₁₉O₆S⁻), OS-267 (C₁₀H₁₉O₆S⁻),
462 OS-281 (C₁₀H₁₇O₇S⁻), OS-299 (C₁₀H₁₉O₈S⁻), OS-307 (C₁₂H₁₉O₇S⁻) and OS-311
463 (C₁₀H₁₅O₉S⁻) have been recently identified in ambient aerosol collected from the major urban
464 locations Shanghai and Hong Kong (Tao et al., 2014; Kuang et al., 2015; Wang et al., 2015).
465 In the absence of retention times and chromatographic conditions, OS isobars such as OS-249
466 or OS-279, which are currently assigned to biogenic-derived OSs (Ma et al., 2014), could also
467 arise from anthropogenic sources such as photooxidation of cyclodecane, especially in urban
468 areas.

469
470
471



472

473 **4. Conclusions**

474 The present study demonstrates the formation of OSs from the photooxidation of alkanes and
475 complements the smog chamber study on formation of OSs and sulfonates from
476 photooxidation of PAHs (Riva et al., 2015a). Together, the results strongly support the
477 importance of the contribution of anthropogenic precursors to OS in ambient urban PM_{2.5}
478 proposed on the basis of aromatic and aliphatic OSs in fine aerosol collected from several
479 major urban locations (Kundu et al., 2013, Tao et al., 2014). Chemical characterization of OSs
480 that were identified in SOA arising from the photooxidation of alkanes were performed and
481 tentative structures have been proposed for OSs identified from the photooxidation of decalin,
482 cyclodecane and dodecane based on composition from exact mass measurement, DBE
483 calculations and the transformations expected from hydroxyl radical oxidation dominated by
484 RO₂/HO₂ chemistry. Enhancement of OS yields in the presence of acidified ammonium
485 sulfate seed is consistent with reactive uptake of gas-phase epoxides as the pathway for OS
486 formation. As previously proposed for IEPOX formation (Paulot et al. 2009), isomerization of
487 RO₂ species to β hydroperoxy alky radicals followed by elimination of OH, is a plausible
488 pathway to gas-phase epoxides. However, more work is required to validate pathway(s)
489 leading to the formation of gaseous epoxy-products. Of critical importance would be
490 investigations starting from authentic primary or secondary oxidation products suggested in
491 this study as putative intermediates to validate the proposed mechanisms. A novel pathway
492 involving reactive uptake of hydroperoxides followed by hydrolysis/sulfation reactions is
493 proposed to explain the formation of OS-279 (C₁₂H₂₃O₅S⁻); however, more work is also
494 required to examine how acidified sulfate seed aerosols take up organic peroxides from the
495 gas phase and how particle-phase reactions might degrade organic peroxides into low-
496 volatility products such as the OSs.

497



498 **Acknowledgments**

499 The authors thank the Camille and Henry Dreyfus Postdoctoral Fellowship Program in
500 Environmental Chemistry for their financial support. The authors wish also to thank CAPES
501 Foundation, Ministry of Education of Brazil (award no. 99999.000542/2015-06) for their
502 financial support. This study was supported in part by the National Oceanic and Atmospheric
503 Administration (NOAA) Climate Program Office's AC4 program, award no.
504 NA13OAR4310064. The authors wish to thank Kasper Kristensen and Marianne Glasius
505 (Department of Chemistry, Aarhus University, Denmark) who synthesized the 3-pinanol-2-
506 hydrogen sulfate. The authors also thank Tauseef Quraishi, Abid Mahmood, and James
507 Shauer for providing filters collected in Lahore, in addition to the Government of Pakistan,
508 the Pakistani Higher Education Commission, and the United States Agency for International
509 Development (US-AID) for funding field sample collection in Pakistan.

510

511



512 **References**

- 513 Atkinson, R.: Atmospheric chemistry of VOCs and NO_x, *Atmos. Environ.*, **34**, 2063-2101, 2000.
- 514
- 515 Altieri, K.E., Turpin, B.J., and Seitzinger, S.P.: Oligomers, organosulfates, and nitrooxy
516 organosulfates in rainwater identified by ultra-high resolution electrospray ionization FT-ICR mass
517 spectrometry, *Atmos. Chem. Phys.*, **9**, 2533-2542, 2009.
- 518
- 519 Attygalle, A.B., Garcia-Rubio, S., Ta, J., and Meinwald, J.: Collisionally-induced dissociation mass
520 spectra of organic sulfate anions, *J. Chem. Soc., Perkin Trans. 2*, **4**, 498-506, 2001.
- 521
- 522 Boone, E.J., Laskin, A., Laskin, J., Wirth, C., Shepson, P.B., Stirm, B.H., and Pratt, K.A.: Aqueous
523 processing of atmospheric organic particles in cloud water collected via aircraft sampling, *Environ.*
524 *Sci. Technol.*, **49**, 8523-8530, 2015.
- 525
- 526 Carrasquillo, A.J., Hunter, J.F., Daumit, K.E., and Kroll, J.H.: Secondary organic aerosol formation
527 via the isolation of individual reactive intermediates: role of alkoxy radical structure, *J. Phys. Chem.*
528 *A*, **118**, 8807-8816, 2014.
- 529
- 530 Chacon-Madrid, H.J., Henry, K.M., and Donahue, N.M.: Photo-oxidation of pinonaldehyde at low
531 NO_x: from chemistry to organic aerosol formation, *Atmos. Chem. Phys.*, **13**, 3227-3236, 2013.
- 532
- 533 Chan, M.N., Surratt, J.D., Chan, A.W.H., Schilling, K., Offenberg, J.H., Lewandowski, M., Edney,
534 E.O., Kleindienst, T.E., Jaoui, M., Edgerton, E.S., Tanner, R.L., Shaw, S.L., Zheng, M., Knipping,
535 E.M., and Seinfeld, J.H.: Influence of aerosol acidity on the chemical composition of secondary
536 organic aerosol from β -caryophyllene, *Atmos. Chem. Phys.*, **11**, 1735-1751, 2011.
- 537
- 538 Claeys, M., Wang, W., Ion, A.C., Kourtchev, I., Gelencsér, A., and Maenhaut, W.: Formation of
539 secondary organic aerosols from isoprene and its gas-phase oxidation products through reaction with
540 hydrogen peroxide, *Atmos. Environ.*, **38**, 4093-4098, 2004.
- 541
- 542 Darer, A.I., Cole-Filipiak, N.C., O'Connor, A.E., and Elrod, M.J.: Formation and stability of
543 atmospherically relevant isoprene-derived organosulfates and organonitrates, *Environ. Sci. Technol.*,
544 **45**, 1895-1902, 2011.
- 545
- 546 Ehn, M., Thornton, J.A., Kleist, E., Sipilä, M., Junninen, H., Pullinen, I., Springer, M., Rubach, F.,
547 Tillmann, R., Lee, B., Lopez-Hilfiker, F., Andres, S., Acir, I.-H., Rissanen, M., Jokinen, T.,



- 548 Schobesberger, S., Kangasluoma, J., Kontkanen, J., Nieminen, T., Kurten, T., Nielsen, L.B.,
549 Jorgensen, S., Kjaergaard, H.G., Canagaratna, M., Maso, M.D., Berndt, T., Petaja, T., Wahner, A.,
550 Kerminen, V.-M., Kulmala, M., Worsnop, D.R., Wildt, J., and Mentel, T.F.: A large source of low-
551 volatility secondary organic aerosol, *Nature*, 506, 476–479, 2014.
- 552
- 553 Elder, A., and Oberdörster, G.: Translocation and effects of ultrafine particles outside of the lung,
554 *Clin. Occup. Environ. Med.*, 5, 785-796, 2006.
- 555
- 556 Fraser, M.P., Cass, G.R., Simoneit, B.R.T., and Rasmussen, R.A.: Air quality model evaluation data
557 for organics. 4. C2-C36 non- aromatic hydrocarbons, *Environ. Sci. Technol.*, 31, 2356-2367, 1997.
- 558
- 559 Gaston, C.J., Riedel, T.P., Zhang, Z., Gold, A., Surratt, J.D., and Thornton, J.A: Reactive uptake of an
560 isoprene-derived epoxydiol to submicron aerosol particles, *Environ. Sci. Technol.*, 48, 11178-11186,
561 2014.
- 562
- 563 Gentner, D.R., Isaacman, G., Worton, D.R., Chan, A.W.H., Dallmann, T.R., Davis, L., Liu, S., Day,
564 D.A., Russell, L.M., Wilson, K.R., Weber, R., Guha, A., Harley, R.A., and Goldstein, A.H.:
565 Elucidating secondary organic aerosol from diesel and gasoline vehicles through detailed
566 characterization of organic carbon emissions. *Proc. Natl. Acad. Sci.*, 109, 18318–18323, 2012.
- 567
- 568 Gómez-González, Y., Surratt, J.D., Cuyckens, F., Szmigielski, R., Vermeylen, R., Jaoui, M.,
569 Lewandowski, M., Offenberg, J.H., Kleindienst, T.E., Edney, E.O., Blockhuys, F., Van Alsenoy, C.,
570 Maenhaut, W., and Claeys, M.: Characterization of organosulfates from the photooxidation of
571 isoprene and unsaturated fatty acids in ambient aerosol using liquid chromatography/(-) electrospray
572 ionization mass spectrometry, *J. Mass Spect.*, 43, 371-382, 2008.
- 573
- 574 Hallquist, M., Wenger, J.C., Baltensperger, U., Rudich, Y., Simpson, D., Claeys, M., Dommen, J.,
575 Donahue, N.M., George, C., Goldstein, A.H., Hamilton, J.F., Herrmann, H., Hoffmann, T., Iinuma, Y.,
576 Jang, M., Jenkin, M.E., Jimenez, J.L., Kiendler-Scharr, A., Maenhaut, W., McFiggans, G., Mentel,
577 T.F., Monod, A., Prévôt, A.S.H., Seinfeld, J.H., Surratt, J.D., Szmigielski, R., and Wildt, J.: The
578 formation, properties and impact of secondary organic aerosol: current and emerging issues, *Atmos.*
579 *Chem. Phys.*, 9, 5155-5236, 2009.
- 580
- 581 Hansen, A.M.K., Kristensen, K., Nguyen, Q.T., Zare, A., Cozzi, F., Nøjgaard, J.K., Skov, H., Brandt,
582 J., Christensen, J.H., Ström, J., Tunved, P., Krejci, R., and Glasius, M.: Organosulfates and organic
583 acids in Arctic aerosols: Speciation, annual variation and concentration levels, *Atmos. Chem. Phys.*,
584 14, 7807-7823, 2014.



- 585 Hatch, L.E., Creamean, J.M., Ault, A.P., Surratt, J.D., Chan, M.N., Seinfeld, J.H., Edgerton, E.S., Su,
586 Y., and Prather, K.A.: Measurements of isoprene-derived organosulfates in ambient aerosols by
587 aerosol time-of-flight mass spectrometry - Part 1: Single particle atmospheric observations in Atlanta,
588 Environ. Sci. Technol., 45, 5105-5111.
589
- 590 Hayes, P.L., Ortega, A.M., Cubison, M.J., Froyd, K.D., Zhao, Y., Cliff, S.S., Hu, W.W., Toohey,
591 D.W., Flynn, J.H., Lefer, B.L., Grossberg, N., Alvarez, S., Rappenglück, B., Taylor, J.W., Allan, J.D.,
592 Holloway, J.S., Gilman, J.B., Kuster, W.C., De Gouw, J.A., Massoli, P., Zhang, X., Liu, J., Weber,
593 R.J., Corrigan, A.L., Russell, L.M., Isaacman, G., Worton, D.R., Kreisberg, N.M., Goldstein, A.H.,
594 Thalman, R., Waxman, E.M., Volkamer, R., Lin, Y.H., Surratt, J.D., Kleindienst, T.E., Offenberg,
595 J.H., Dusanter, S., Griffith, S., Stevens, P.S., Brioude, J., Angevine, W.M., and Jimenez, J.L.: Organic
596 aerosol composition and sources in Pasadena, California, during the 2010 CalNex campaign, J.
597 Geophys. Res. Atmos., 118, 9233-9257, 2013.
598
- 599 Hawkins, L.N., Russell, L.M., Covert, D. S., Quinn, P. K., and Bates, T. S.: Carboxylic acids, sulfates,
600 and organosulfates in processed continental organic aerosol over the south east Pacific Ocean during
601 VOCALS-REx 2008, J. Geophys. Res.-Atmos., 115, D13201, 2010.
602
- 603 Hu, K.S., Darer, A.I., and Elrod, M.J.: Thermodynamics and kinetics of the hydrolysis of
604 atmospherically relevant organonitrates and organosulfates, Atmos. Chem. Phys., 11, 8307–8320,
605 2011.
606
- 607 Hunter, J.F., Carrasquillo, A.J., Daumit, K.E., and Kroll, J.H.: Secondary organic aerosol formation
608 from acyclic, monocyclic, and polycyclic alkanes, Environ. Sci. Technol., 48, 10227-10234, 2014.
609
- 610 Iinuma, Y., Müller, C., Berndt, T., Böge, O., Claeys, M., and Herrmann, H.: Evidence for the
611 existence of organosulfates from β -pinene ozonolysis in ambient secondary organic aerosol, Environ.
612 Sci. Tech., 41, 6678-6683, 2007.
613
- 614 Iinuma, Y., Böge, O., Kahnt, A., and Herrmann, H.: Laboratory chamber studies on the formation of
615 organosulfates from reactive uptake of monoterpene oxides, Phys. Chem. Chem. Phys., 11, 7985-
616 7997, 2009.
617
- 618 Jacobs, M.I., Darer, A.I., and Elrod, M.J.: Rate constants and products of the OH reaction with
619 isoprene-derived epoxides, Environ. Sci. Technol, 43, 12868-12876, 2013.
620



- 621 Jokinen, T., Sipilä, M., Richters, S., Kerminen, V.-M., Paasonen, P., Stratmann, F., Worsnop, D.,
622 Kulmala, M., Ehn, M., Herrmann, H., and Berndt, T.: Rapid Autoxidation Forms Highly Oxidized
623 RO₂ Radicals in the Atmosphere, *Angew. Chem. Internat. Ed.*, 53, 14596–14600, 2014.
- 624
- 625 Kamens, R.M., Zhang, H., Chen, E.H., Zhou, Y., Parikh, H.M., Wilson, R.L., Galloway, K.E., and
626 Rosen, E.P.: Secondary organic aerosol formation from toluene in an atmospheric hydrocarbon
627 mixture: water and particle seed effects, *Atmos. Environ.*, 45, 2324-2334, 2011.
- 628
- 629 Kitanovski, Z., Grgic, I., Yasmeen, F., Claeys, M., and Cusak, A.: Development of a liquid
630 chromatographic method based on ultraviolet–visible and electrospray ionization mass spectrometric
631 detection for the identification of nitrocatechols and related tracers in biomass burning atmospheric
632 organic aerosol, *Rapid Commun. Mass. Spectrom.*, 26, 793-804, 2012.
- 633
- 634 Kristensen, K., and Glasius, M.: Organosulfates and oxidation products from biogenic hydrocarbons in
635 fine aerosols from a forest in North West Europe during spring, *Atmos. Environ.*, 45, 4546-4556,
636 2011.
- 637
- 638 Kroll, J.H., and Seinfeld, J.H.: Chemistry of secondary organic aerosol: formation and evolution of
639 low-volatility organics in the atmosphere, *Atmos. Environ.*, 42, 3593-3624, 2008.
- 640
- 641 Kuang, B.Y., Lin, P., Hub, M., and Yu, J.Z.: Aerosol size distribution characteristics of organosulfates
642 in the Pearl River Delta region, China, *Atmos. Environ.*, In Press, 2015.
- 643
- 644 Kundu, S., Quraishi, T.A., Yu, G., Suarez, C., Keutsch, F.N., and Stone, E.A.: Evidence and
645 quantification of aromatic organosulfates in ambient aerosols in Lahore, Pakistan, *Atmos. Chem.*
646 *Phys.*, 13, 4865-4875, 2013.
- 647
- 648 Kwok, E.S.C., and Atkinson, R.: Estimation of hydroxyl radical reaction rate constants for gas-phase
649 organic compounds using a structure-reactivity relationship: an update, *Atmos. Environ.*, 29, 1685-
650 1695, 1995.
- 651
- 652 Loza, C.L., Craven, J.S., Yee, L.D., Coggon, M.M., Schwantes, R.H., Shiraiwa, M., Zhang, X.,
653 Schilling, K.A., Ng, N.L., Canagaratna, M.R., Ziemann, P., Flagan, R.C., and Seinfeld, J.H.:
654 Secondary organic aerosol yields of 12-carbon alkanes, *Atmos. Chem. Phys.*, 7, 1423-1439, 2014.
- 655
- 656 Lee, S., Jang, M., and Kamens, R. K.: SOA formation from the photooxidation of α -pinene in the
657 presence of freshly emitted diesel soot exhaust, *Atmos. Environ.*, 38, 2597–2605, 2004.



- 658 Liao, J., Froyd, K.D., Murphy, D.M., Keutsch, F.N., Yu, G., Wennberg, P.O., St. Clair, J.M., Crouse,
659 J.D., Wisthaler, A., Mikoviny, T., Jimenez, J.L., Campuzano-Jost, P., Day, D.A., Hu, W., Ryerson,
660 T.B., Pollack, I.B., Peischl, J., Anderson, B.E., Ziemba, L.D., Blake, D.R., Meinardi, S., and Diskin,
661 G.: Airborne measurements of organosulfates over the continental U.S., *J. Geophys. Res. D*, 120,
662 2990-3005, 2015.
- 663
- 664 Liggio, J., and Li, S.-M.: Organosulfate formation during the uptake of pinonaldehyde on acidic
665 sulfate aerosols, *Geophys. Res. Lett.*, 33, L13808, 2006.
- 666
- 667 Lim, Y.B., and Ziemann, P.J.: Products and mechanism of secondary organic aerosol formation from
668 reactions of n-alkanes with OH radicals in the presence of NO_x, *Environ. Sci. Technol.*, 39, 9229-
669 9236, 2005.
- 670
- 671 Lim, Y.B., and Ziemann, P.J.: Effects of molecular structure on aerosol yields from OH radical-
672 initiated reactions of linear, branched, and cyclic alkanes in the presence of NO_x, *Environ. Sci.*
673 *Technol.*, 43, 2328-2334, 2009.
- 674
- 675 Lin, Y.-H., Zhang, Z., Docherty, K.S., Zhang, H., Budisulistiorini, S.H., Rubitschun, C.L., Shaw, S.L.,
676 Knipping, E.M., Edgerton, E.S., Kleindienst, T.E., Gold, A., and Surratt, J.D.: Isoprene epoxydiols as
677 precursors to secondary organic aerosol formation: acid-catalyzed reactive uptake studies with
678 authentic compounds, *Environ. Sci. Technol.*, 46, 250-258, 2012.
- 679
- 680 Lin, Y.-H., Budisulistiorini, S.H., Chu, K., Siejack, R.A., Zhang, H., Riva, M., Zhang, Z., Gold, A.,
681 Kautzman, K.E., and Surratt, J.D.: Light-absorbing oligomer formation in secondary organic aerosol
682 from reactive uptake of isoprene epoxydiols, *Environ. Sci. Technol.*, 48, 12012-12021, 2014.
- 683
- 684 Ma, Y., Xu, X., Song, W., Geng, F., and Wang, L.: Seasonal and diurnal variations of particulate
685 organosulfates in urban Shanghai, China, *Atmos. Environ.*, 85, 152-160, 2014.
- 686
- 687 Mael, L.E., Jacobs, M.I., and Elrod, M.J.: Organosulfate and nitrate formation and reactivity from
688 epoxides derived from 2-methyl-3-buten-2-ol, *J. Phys. Chem. A*, 119, 4464-4472, 2015.
- 689
- 690 Mentel, T.F., Springer, M., Ehn, M., Kleist, E., Pullinen, I., Kurten, T., Rissanen, M., Wahner, A., and
691 Wildt, J.: Formation of highly oxidized multifunctional compounds: autoxidation of peroxy radicals
692 formed in the ozonolysis of alkenes –deduced from structure–product relationships, *Atmos. Chem.*
693 *Phys.*, 15, 6745-6765, 2015.
- 694



- 695 Mutzel, A., Poulain, L., Berndt, T., Iinuma, Y., Rodigast, M., Böge, O., Richters, S., Spindler, G.,
696 Sipila, M., Jokinen, T., Kulmala, M., and Herrmann, H.: Highly oxidized multifunctional organic
697 compounds observed in tropospheric particles: a field and laboratory study, *Environ. Sci. Technol.*, 49,
698 7754-7761, 2015.
- 699
- 700 Ng, N.L., Kwan, A.J., Surratt, J.D., Chan, A.W.H., Chhabra, P.S., Sorooshian, A., Pye, H.O.T.,
701 Crounse, J.D., Wennberg, P.O., Flagan, R.C., and Seinfeld, J.H.: Secondary organic aerosol (SOA)
702 formation from reaction of isoprene with nitrate radicals (NO₃), *Atmos. Chem. Phys.*, 8, 4117-4140,
703 2008.
- 704
- 705 Nozière, B., Ekström, S., Alsberg, T., and Holmström, S.: Radical-initiated formation of
706 organosulfates and surfactants in atmospheric aerosols, *Geophys. Res. Lett.*, 37, L05806, 2010.
- 707
- 708 Paulot, F., Crounse, J.D., Kjaergaard, H.G., Kroll, J.H., Seinfeld, J.H., and Wennberg, P.O.: Isoprene
709 photooxidation: New insights into the production of acids and organic nitrates, *Atmos. Chem. Phys.*,
710 9, 1479-1501, 2009.
- 711
- 712 Pratt, K.A., Fiddler, M.N., Shepson, P.B., Carlton, A.G, and Surratt, J.D.: Organosulfates in cloud
713 water above the Ozarks isoprene source region, *Atmos. Environ.*, 77, 231-238, 2013.
- 714
- 715 Presto, A.A., Miracolo, M.A., Donahue, N.M., and Robinson, A.L.: Secondary organic aerosol
716 formation from high-NO_x Photo-oxidation of low volatility precursors: N-alkanes, *Environ. Sci.*
717 *Technol.*, 44, 2029-2034, 2010
- 718
- 719 Pye, H.O.T., and Pouliot, G.A.: Modeling the role of alkanes, polycyclic aromatic hydrocarbons, and
720 their oligomers in secondary organic aerosol formation, *Environ. Sci. Technol.*, 46, 6041-6047, 2012.
- 721
- 722 Raff, J.D., and Finlayson-Pitts, B.J.: Hydroxyl radical quantum yields from isopropyl nitrite photolysis
723 in air, *Environ. Sci. Technol.*, 44, 8150-8155, 2010.
- 724
- 725 Riedel, T.P., Lin, Y., Budisulistiorini, S.H., Gaston, C.J., Thornton, J.A., Zhang, Z., Vizuete, W.,
726 Gold, D., and Surratt, J.D.: Heterogeneous reactions of isoprene-derived epoxides: reaction
727 probabilities and molar secondary organic aerosol yield estimates, *Environ. Sci. Technol. Lett.*, 2, 38-
728 42, 2015.
- 729
- 730 Riva, M., Tomaz, S., Cui, T., Lin, Y.-H., Perraudin, E., Gold, A., Stone, E.A., Villenave, E., and
731 Surratt, J.D.: Evidence for an unrecognized secondary anthropogenic source of organosulfates and



- 732 sulfonates: Gas-phase oxidation of polycyclic aromatic hydrocarbons in the presence of sulfate
733 aerosol, *Environ. Sci. Technol.*, 49, 6654–6664, 2015a.
734
- 735 Riva, M., Budisulistiorini, S.H., Zhang, Z., Gold, A., and Surratt, J.D.: Chemical characterization of
736 secondary organic aerosol constituents from isoprene ozonolysis in the presence of acidic aerosol,
737 *Atmos. Chem.*, In Press, 2015b.
738
- 739 Romero, F., and Oehme, M.: Organosulfates – a new component of humic-like substances in
740 atmospheric aerosols?, *J. Atmos. Chem.*, 52, 283-294, 2005.
741
- 742 Rudzinski, K. J., Gmachowski, L., and Kuznietsova, I.: Reactions of isoprene and sulphony radical-
743 anions – a possible source of atmospheric organosulphites and organosulphates, *Atmos. Chem. Phys.*,
744 9, 2129-2140, 2009.
745
- 746 Ruehl, C. R., Nah, T. Isaacman, G., Worton, D. R., Chan, A. W. H., Kolesar, K. R., Cappa, C. D.,
747 Goldstein, A. H., and Wilson, K. R.: The influence of molecular structure and aerosol phase on the
748 heterogeneous oxidation of normal and branched alkanes by OH, *J. Phys. Chem. A*, 117, 3990-4000,
749 2013.
750
- 751 Schilling Fahnestock, K.A., Yee, L.D., Loza, C.L., Coggon, M.M., Schwantes, R., Zhang, X.,
752 Dalleska, N.F., and Seinfeld, J.H.: Secondary organic aerosol composition from C12 alkanes, *J. Phys.*
753 *Chem. A*, 119, 4281-4297, 2015.
754
- 755 Schindelka, J., Iinuma, Y., Hoffmann, D., and Herrmann, H.: Sulfate radical-initiated formation of
756 isoprene-derived organosulfates in atmospheric aerosols, *Faraday Discuss.*, 165, 237-259, 2013.
757
- 758 Schöne, L., Schindelka, J., Szeremeta, E., Schaefer, T., Hoffmann, D., Rudzinski, K.J., Szmigielski,
759 R., and Herrmann, H.: Atmospheric aqueous phase radical chemistry of the isoprene oxidation
760 products methacrolein, methyl vinyl ketone, methacrylic acid and acrylic acid – kinetics and product
761 studies, *Phys. Chem. Chem. Phys.*, 16, 6257–6272, 2014
762
- 763 Shalamzari, S.M., Ryabtsova, O., Kahnt, A., Vermeylen, R., Hérent, M.-F., Quetin-Leclercq, J., Van
764 Der Veken, P., Maenhaut, W., and Claeys, M.: Mass spectrometric characterization of organosulfates
765 related to secondary organic aerosol from isoprene, *Rapid Commun. Mass Spectrom.*, 27, 784-794,
766 2013.
767
- 768 Shalamzari, M.S., Kahnt, A., Vermeylen, R., Kleindienst, T.E., Lewandowski, M., Cuyckens, F.,



- 769 Maenhaut, W., and Claeys, M.: Characterization of polar organosulfates in secondary organic aerosol
770 from the green leaf volatile 3-Z-hexenal, *Environ. Sci. Technol.*, 48, 12671–12678, 2014.
771
- 772 Shalamzari, M.S., Vermeylen, R., Blockhuys, F., Kleindienst, T.E., Lewandowski, M., Szmigielski,
773 R., Rudzinski, K.J., Spolnik, G., Danikiewicz, W., Maenhaut, W., and Claeys, M.: Characterization of
774 polar organosulfates in secondary organic aerosol from the unsaturated aldehydes 2-E-pentenal, 2-E-
775 hexenal, and 3-Z-hexenal, *Atmos. Chem. Phys. Discuss.*, 15, 29555–29590, 2015.
776
- 777 Stevens, B., and Boucher, O.: The aerosol effect, *Nature*, 490, 40–41, 2012.
778
- 779 Stone, E., Schauer, J., Quraishi, T.A., and Mahmood, A.: Chemical characterization and source
780 apportionment of fine and coarse particulate matter in Lahore, Pakistan, *Atmos. Environ.*, 44, 1062-
781 1070, 2010.
782
- 783 Stone, E.A., Yang, L., Yu, L.E., and Rupakheti, M.: Characterization of organosulfate in atmospheric
784 aerosols at Four Asian locations, *Atmos. Environ.*, 47, 323–329, 2012.
785
- 786 Surratt, J.D., Kroll, J.H., Kleindienst, T.E., Edney, E.O., Claeys, M., Sorooshian, A., Ng, N.L.,
787 Offenberg, J.H., Lewandowski, M., Jaoui, M., Flagan, R.C., and Seinfeld, J.H.: Evidence for
788 organosulfates in secondary organic aerosol, *Environ. Sci. Technol.*, 41, 517–527, 2007.
789
- 790 Surratt, J.D., Gómez-González, Y., Chan, A.W.H., Vermeylen, R., Shahgholi, M., Kleindienst, T.E.,
791 Edney, E.O., Offenberg, J.H., Lewandowski, M., Jaoui, M., Maenhaut, W., Claeys, M., Flagan, R.C.,
792 and Seinfeld, J.H.: Organosulfate formation in biogenic secondary organic aerosol, *J. Phys. Chem. A*,
793 112, 8345–8378, 2008.
794
- 795 Surratt, J.D., Chan, A.W.H., Eddingsaas, N.C., Chan, M., Loza, C.L., Kwan, A.J., Hersey, S.P.,
796 Flagan, R.C., Wennberg, P.O., and Seinfeld, J.H.: Reactive intermediates revealed in secondary
797 organic aerosol formation from isoprene, *Proc. Natl. Acad. Sci.*, 107, 6640–6645, 2010.
798
- 799 Tao, S., Lu, X., Levac, N., Bateman, A.P., Nguyen, T.B., Bones, D.L., Nizkorodov, S.A., Laskin, J.,
800 Laskin, A., and Yang, X.: Molecular characterization of organosulfates in organic aerosols from
801 Shanghai and Los Angeles urban areas by nanospray-desorption electrospray ionization high-
802 resolution mass spectrometry, *Environ. Sci. Technol.*, 48 (18), 10993–11001, 2014.
803



- 804 Tkacik, D.S., Presto, A.A., Donahue, N.M., and Robinson, A.L.: Secondary organic aerosol formation
805 from intermediate-volatility organic compounds: cyclic, linear, and branched alkanes, *Environ. Sci.*
806 *Technol.*, 46, 8773-8781, 2012.
- 807
- 808 Tolocka, M.P., and Turpin, B.: Contribution of organosulfur compounds to organic aerosol mass,
809 *Environ. Sci. Technol.*, 46, 7978-7983, 2012.
- 810
- 811 Wang, X.K., Rossignol, S., Ma, Y., Yao, L., Wang, M.Y., Chen, J.M., George, C., and Wang, L.:
812 Identification of particulate organosulfates in three megacities at the middle and lower reaches of the
813 Yangtze River, *Atmos. Chem. Phys. Discuss.*, 15, 21414-21448, 2015.
- 814
- 815 Yee, L.D., Craven, J.S., Loza, C.L., Schilling, K.A., Ng, N.L., Canagaratna, M.R., Ziemann, P.J.,
816 Flagan, R.C., and Seinfeld, J.H.: Secondary organic aerosol formation from low-NO_x photooxidation
817 of dodecane: Evolution of multigeneration gas-phase chemistry and aerosol composition, *J. Phys.*
818 *Chem. A*, 116, 6211-6230, 2012.
- 819
- 820 Yee, L.D., Craven, J.S., Loza, C.L., Schilling, K.A., Ng, N.L., Canagaratna, M.R., Ziemann, P.J.,
821 Flagan, R.C., and Seinfeld, J.H.: Effect of chemical structure on secondary organic aerosol formation
822 from C12 alkanes, *Atmos. Chem. Phys.*, 13, 11121-11140, 2013.
- 823
- 824 Zhang, H., Worton, D.R., Lewandowski, M., Ortega, J., Rubitschun, C.L., Park, J.-H., Kristensen, K.,
825 Campuzano-Jost, P., Day, D.A., Jimenez, J.L., Jaoui, M., Offenberg, J.H., Kleindienst, T.E., Gilman,
826 J., Kuster, W.C., De Gouw, J., Park, C., Schade, G.W., Frossard, A.A., Russell, L., Kaser, L., Jud, W.,
827 Hansel, A., Cappellin, L., Karl, T., Glasius, M., Guenther, A., Goldstein, A.H., Seinfeld, J.H., Gold,
828 A., Kamens, R.M., and Surratt, J.D.: Organosulfates as tracers for secondary organic aerosol (SOA)
829 formation from 2-methyl-3-buten-2-ol (MBO) in the atmosphere, *Environ. Sci. Technol.*, 46, 9437-
830 9446, 2012.
- 831
- 832 Zhang, X., Schwantes, R.H., Coggon, M.M., Loza, C.L., Schilling, K.A., Flagan, R.C., Seinfeld, J.H.:
833 Role of ozone in SOA formation from alkane photooxidation, *Atmos. Phys. Chem.*, 14, 1733-1753,
834 2014
- 835



836 **Table 1.** Summary of outdoor smog chamber conditions used for the photooxidation of long-
 837 chain alkanes using isopropyl nitrite (IPN) as an OH radical precursor.

838

Hydrocarbons (HCs)	Initial [HC] (ppb)	Chamber Side	Seed aerosol	Initial [IPN] (ppb)	T (K)	RH (%)	Final OA mass ($\mu\text{g m}^{-3}$)
Dodecane	412	N	Non-Acidified	215	304-311	49-59	58
	420	S	Acidified	212	305-311	51-63	65
Dodecane	422	N	Non-Acidified	215	302-308	15-20	49
	427	S	Acidified	212	303-308	14-17	53
Dodecane	397	N	Acidified	215	304-309	45-52	52
	409	S	Acidified	212	305-310	15-19	59
Decalin	175	N	Non-Acidified	138	302-309	48-45	204
	180	S	Acidified	136	302-308	51-49	224
Decalin	199	N	Non-Acidified	138	305-306	13-13	200
	204	S	Acidified	136	306-306	13-14	211
Decalin	N.I.	N	Acidified	138	302-306	43-54	245
	N.I.	S	Acidified	136	301-306	9-12	270
Cyclodecane	257	N	Non-Acidified	172	298-301	53-61	218
	263	S	Acidified	170	299-301	52-60	238
Cyclodecane	256	N	Non-Acidified	172	300-303	13-15	177
	261	S	Acidified	170	300-302	13-14	210
Cyclodecane	245	N	Acidified	172	298-300	10-11	259
	250	S	Acidified	170	299-300	51-49	270

839 *N and S design "North chamber" and "South Chamber", respectively; N.I.: No Information.*

840



Table 2. Concentrations (ng m^{-3}) of OSs identified in laboratory-generated dodecane, decalin and cyclodecane SOA and in fine aerosol collected from two urban locations.

[M - H] ⁻	Precursors	Lahore, Pakistan					Pasadena, USA								
		04-30-2007	05-06-2007	05-12-2007	11-02-2007	11-08-2007	05-17-2010	05-18-2010	05-19-2010	05-23-2010	05-24-2010	05-25-2010	05-28-2010	06-11-2010	
$\text{C}_7\text{H}_{13}\text{O}_8\text{S}^-$ (209.0472) ^{a,b}	Dodecane	7.53	6.53	4.24	6.35	9.66	<i>N.d.</i>	<i>N.d.</i>	0.27	0.07	0.10	<i>N.d.</i>	0.09	0.21	
$\text{C}_9\text{H}_{17}\text{O}_8\text{S}^-$ (237.0786) ^{a,b}	Dodecane	9.35	6.81	4.27	7.27	12.40	0.13	0.15	0.30	0.10	0.16	0.16	0.13	0.25	
$\text{C}_{10}\text{H}_{19}\text{O}_8\text{S}^-$ (251.0946) ^{a,c}	Cyclodecane	10.40	7.51	4.08	13.17	20.96	<i>N.d.</i>	<i>N.d.</i>	<i>N.d.</i>	<i>N.d.</i>	<i>N.d.</i>	<i>N.d.</i>	<i>N.d.</i>	<i>N.d.</i>	
$\text{C}_{10}\text{H}_{17}\text{O}_6\text{S}^-$ (265.079) ^{a,c}	Cyclodecane	2.83	2.45	2.15	2.86	7.63	0.18	0.21	0.35	0.14	0.15	0.16	0.15	0.36	
$\text{C}_9\text{H}_{15}\text{O}_7\text{S}^-$ (267.0554) ^{a,c}	Decalin	0.98	1.87	1.93	2.19	6.53	0.21	0.21	0.58	0.11	0.21	0.20	0.16	0.40	
$\text{C}_9\text{H}_{17}\text{O}_7\text{S}^-$ (269.0700) ^{a,b}	Decalin	2.04	3.02	2.22	2.62	7.56	0.42	0.38	0.58	0.26	0.40	0.38	0.35	0.56	
$\text{C}_{10}\text{H}_{15}\text{O}_7\text{S}^-$ (279.0556) ^{a,c}	Cyclodecane	6.38	20.25	21.97	15.06	35.93	0.14	0.21	0.54	0.10	0.19	0.21	0.20	0.29	
$\text{C}_{12}\text{H}_{23}\text{O}_8\text{S}^-$ (279.1272) ^{c,d}	Dodecane	14.57	12.18	3.41	9.50	19.56	<i>N.d.</i>	<i>N.d.</i>	<i>N.d.</i>	<i>N.d.</i>	<i>N.d.</i>	<i>N.d.</i>	<i>N.d.</i>	<i>N.d.</i>	
$\text{C}_9\text{H}_{17}\text{O}_8\text{S}^-$ (285.0651) ^{a,c}	Decalin	<i>N.d.</i>	0.61	<i>N.d.</i>	<i>N.d.</i>	1.44	0.20	0.09	0.21	0.05	0.08	0.09	0.03	0.17	
$\text{C}_{10}\text{H}_{15}\text{O}_8\text{S}^-$ (295.0500) ^{a,c}	Decalin	<i>N.d.</i>	0.53	0.48	0.54	3.78	0.17	0.22	0.65	0.08	0.17	0.24	0.19	0.52	
$\text{C}_{10}\text{H}_{17}\text{O}_8\text{S}^-$ (297.0650) ^{a,c}	Decalin	<i>N.d.</i>	0.78	0.92	0.69	<i>N.d.</i>	0.13	0.08	0.43	0.07	0.10	0.09	0.10	0.24	
$\text{C}_{10}\text{H}_{16}\text{NO}_8\text{S}^-$ (326.0550) ^{a,c}	Decalin	0.25	0.32	0.21	<i>N.d.</i>	<i>N.d.</i>	<i>N.d.</i>	0.13	0.22	0.06	0.09	0.11	0.12	0.11	

^a Quantified using authentic OS (3-pinanol-2-hydrogen sulfate, $\text{C}_9\text{H}_{13}\text{O}_8\text{S}^-$), ^b OSs belonging to group 2, ^c OSs belonging to group 1, ^d quantified using octyl sulfate OS ($\text{C}_8\text{H}_{17}\text{O}_8\text{S}^-$). Different isomers for one ion have been summed; *N.d.*: not detected.

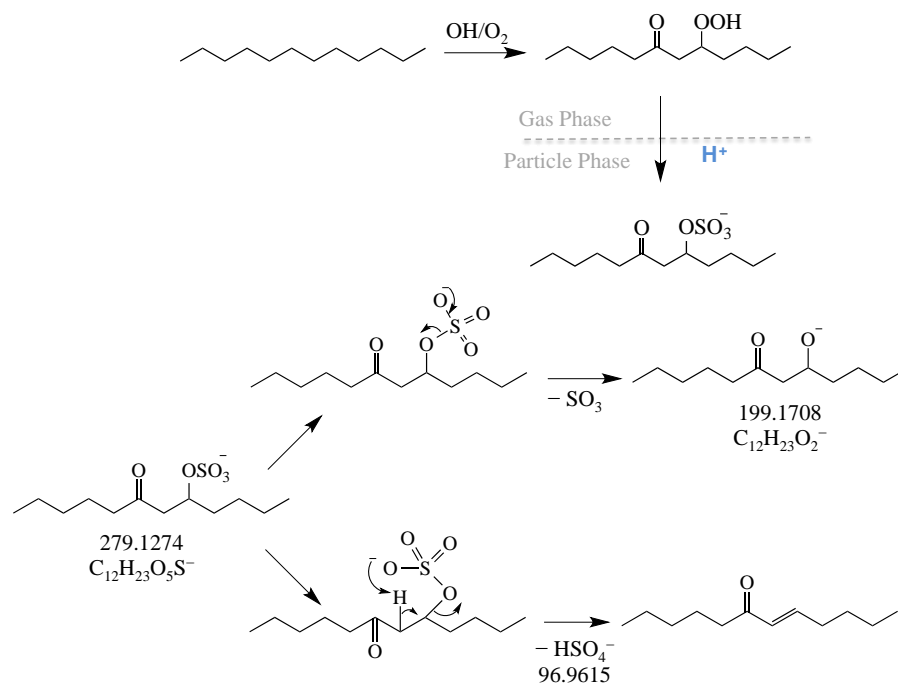


Figure 1. Proposed formation pathway of OS-279 and its corresponding fragmentation routes. The suggested mechanism is based on identified products from previous study (Yee et al., 2012).

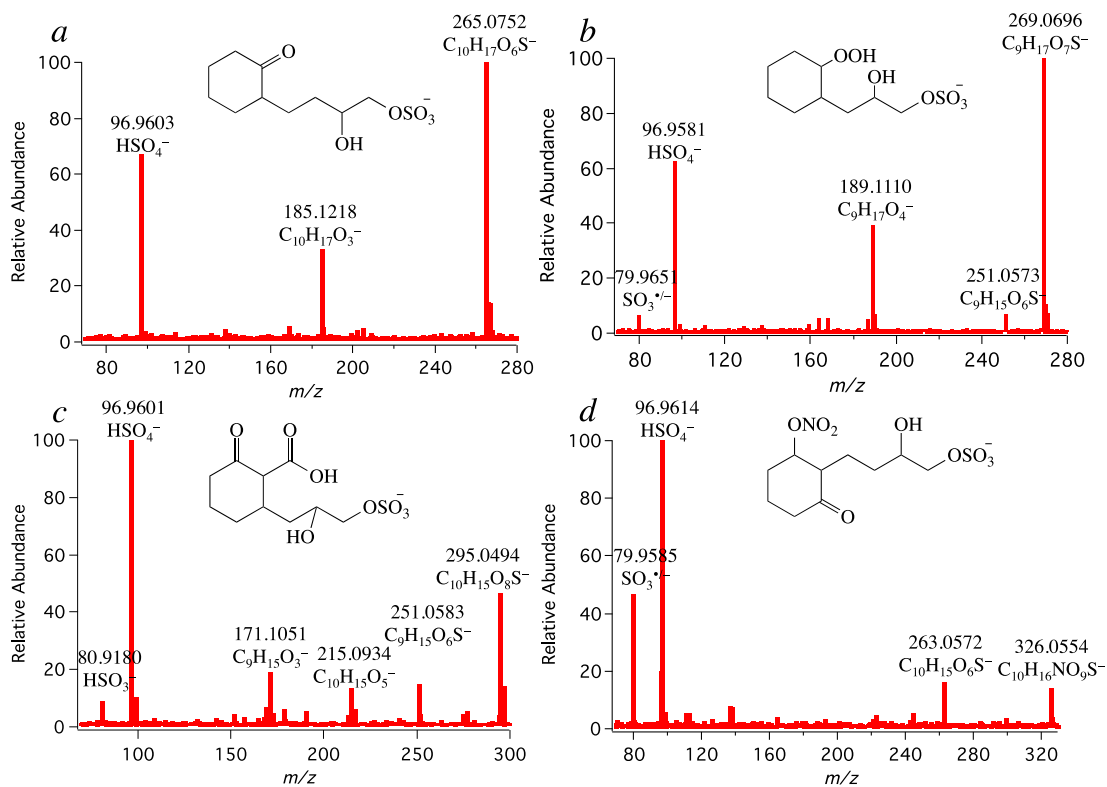


Figure 2. MS² spectra obtained for selected decalin-derived OSs: (a) m/z 265.0752 ($C_{10}H_{17}O_6S^-$), (b) m/z 269.0696 ($C_9H_{17}O_7S^-$), (c) m/z 295.0494 ($C_{10}H_{15}O_8S^-$) and (d) m/z 326.0554 ($C_{10}H_{16}NO_9S^-$). Fragmentation schemes are proposed in Figure S2.

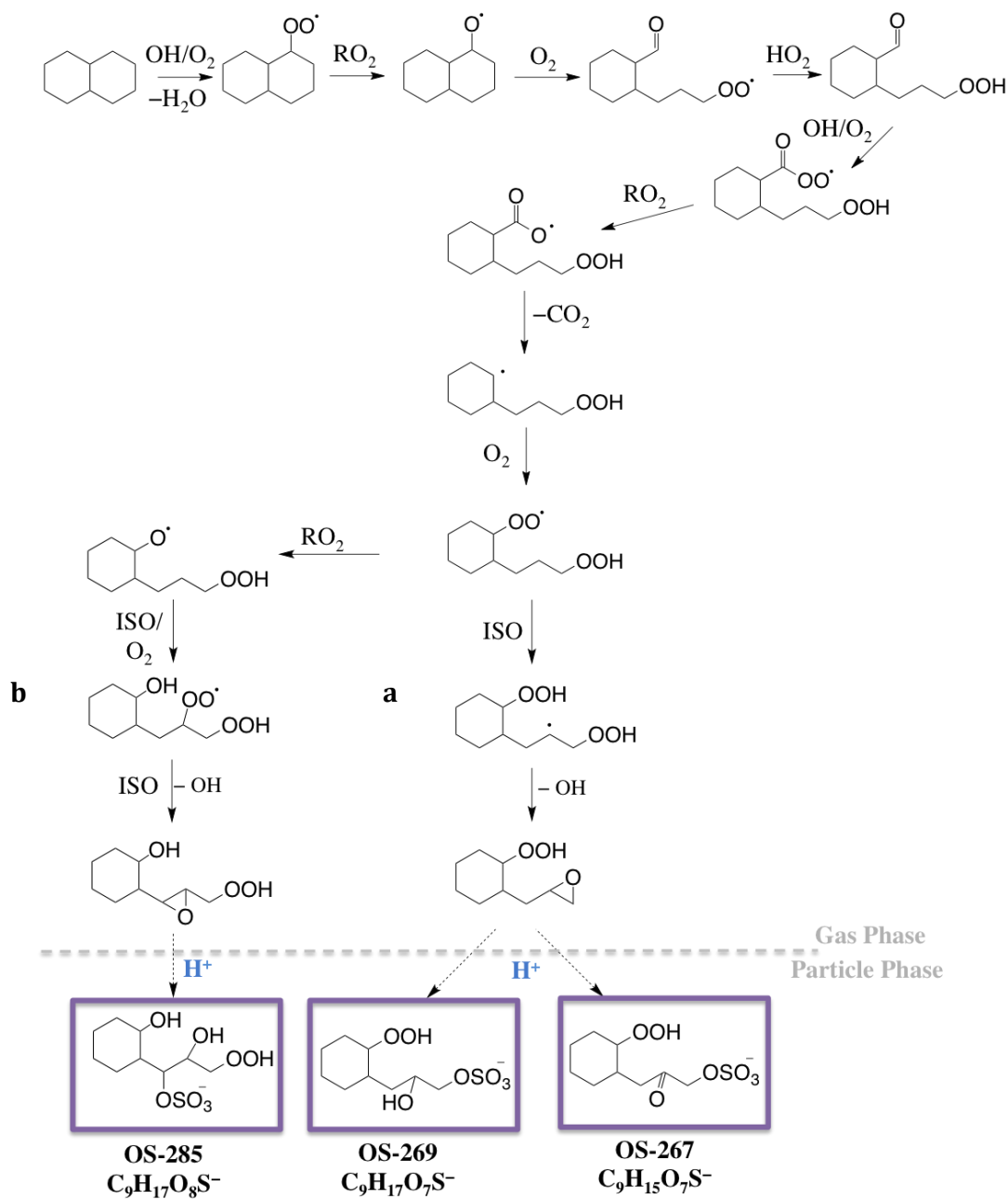


Figure 3. Proposed formation pathways of OS-267, OS-269 and OS-285 from the oxidation of decalin in presence of sulfate aerosol. ISO = isomerization reaction either through H shift (1,5- or 1,7-) or through hydroperoxide isomerization with an R radical.

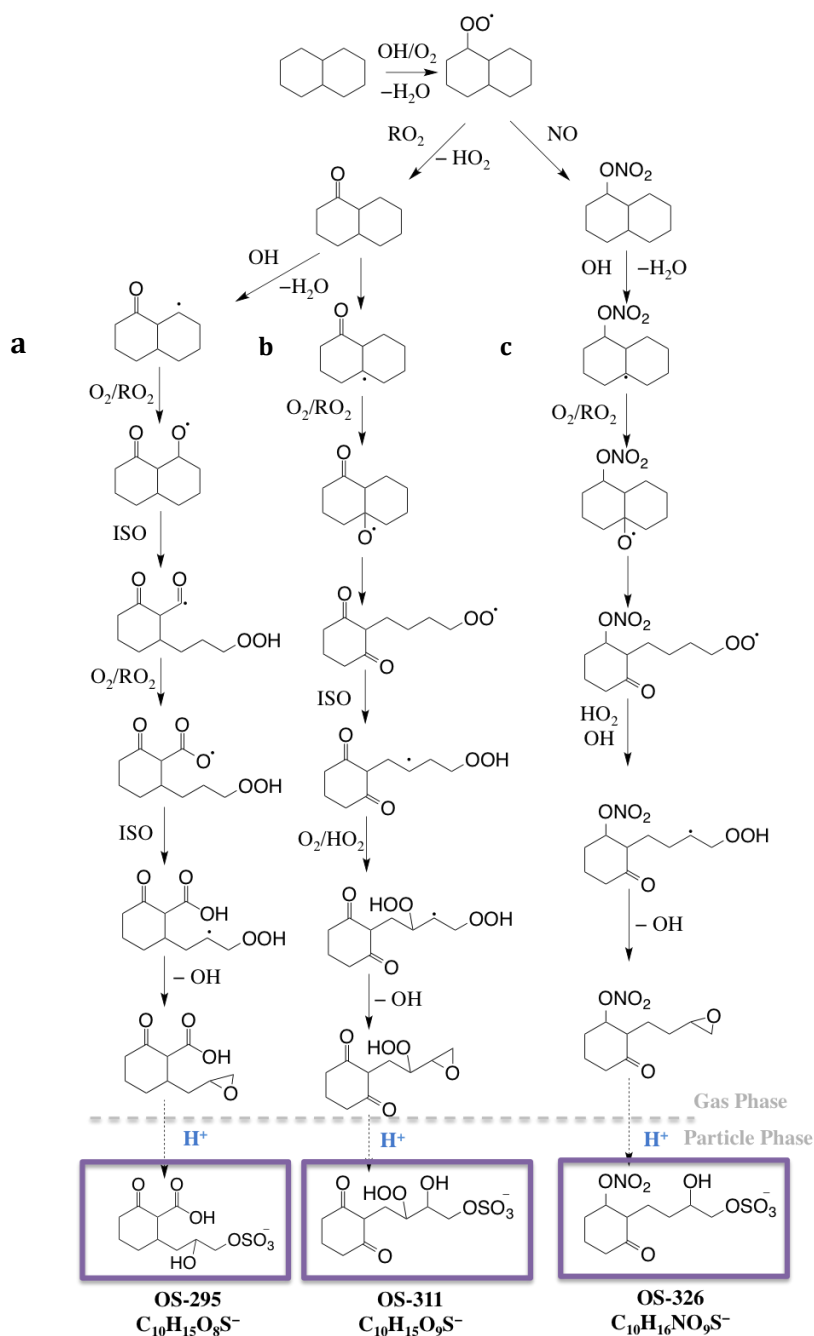


Figure 4. Proposed formation pathways of OS-295, OS-311 and OS-326 from the oxidation of decalin in the presence of sulfate aerosol. ISO = isomerization reaction either through H shift (1,5- or 1,7-) or through hydroperoxide isomerization with an R radical.

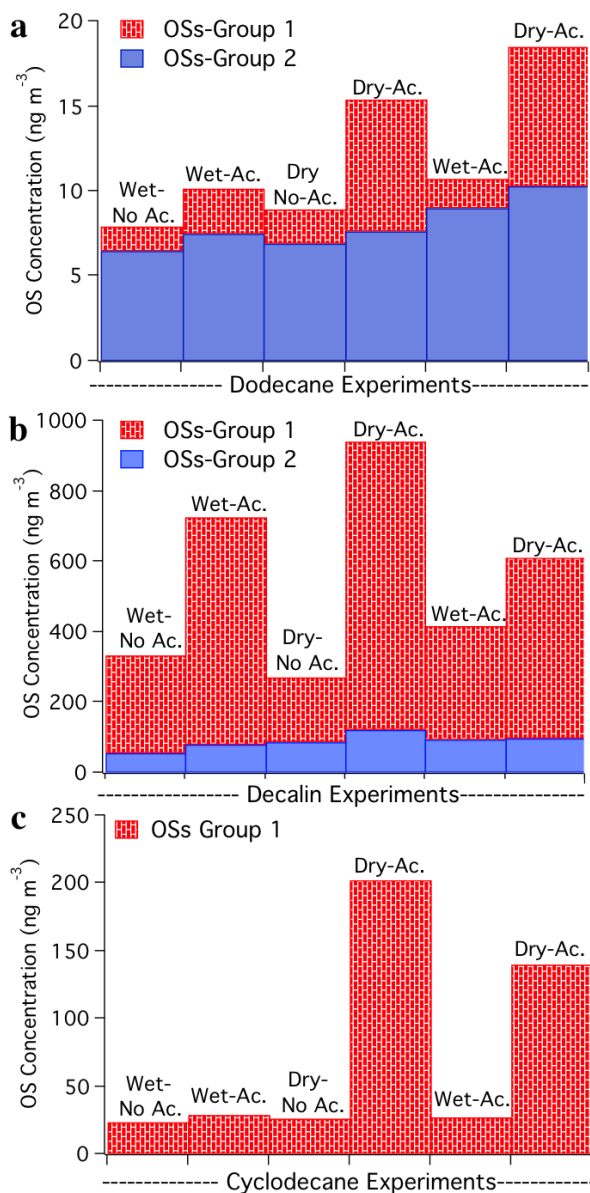


Figure 5. Impact of acidity on OS formation from gas-phase oxidation of (a) dodecane, (b) decalin, and (c) cyclodecane. OSs from Group-1 corresponds to compounds strongly impacted by aerosol acidity, while OSs from Group-2 appeared to have less dependency on aerosol acidity.

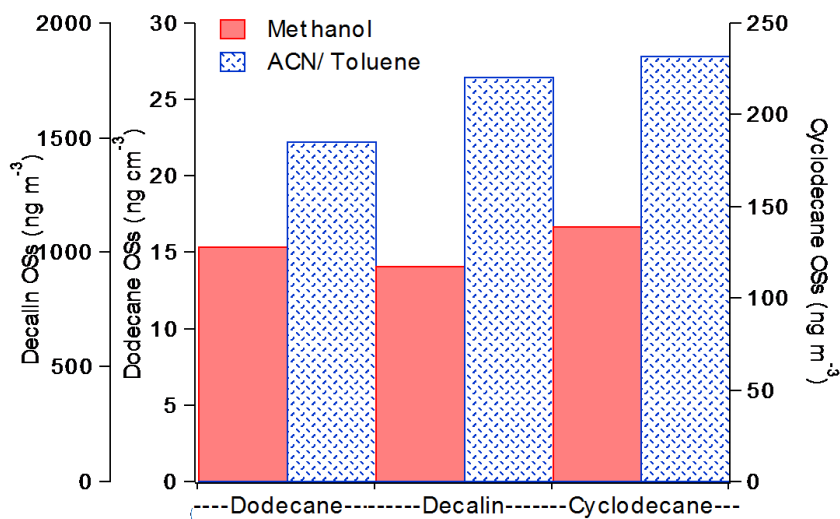


Figure 6. Impact of extraction solvent composition on quantification of identified OSs from gas-phase oxidation of alkanes.

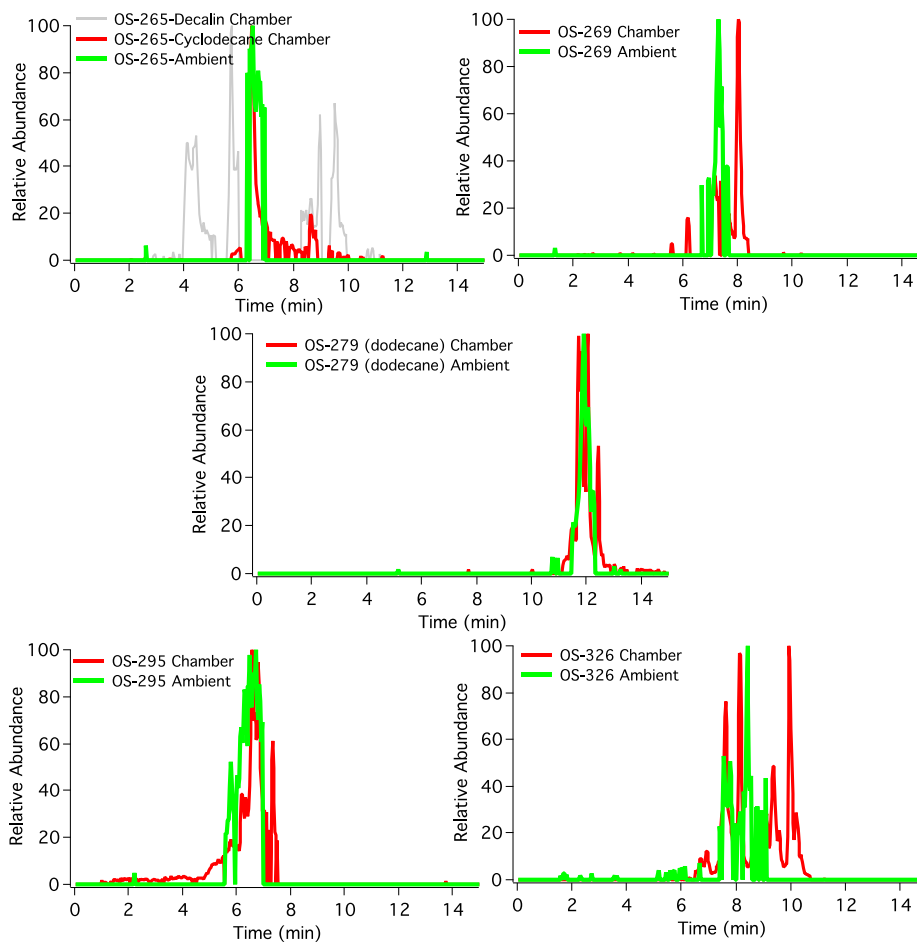


Figure 7. Extracted ion chromatograms (EICs) for selected alkane OSs identified in both smog chamber experiments (in red) and ambient samples (in green).